ELSEVIER

International Journal of Heat and Fluid Flow 21 (2000) 239–251

International Journal of HEAT AND FLUID FLOW

www.elsevier.com/locate/ijhff

Modelling shock-affected near-wall flows with anisotropy-resolving turbulence closures

M.A. Leschziner *, P. Batten, H. Loyau

Department of Mechanical Engineering, UMIST, P.O. Box 88, Manchester M60 1QD, UK

Received 1 September 1999; accepted 13 February 2000

Abstract

This paper reviews some recent research aiming to assess the performance of advanced forms of second-moment closure and non-linear eddy-viscosity models for compressible flows, with particular emphasis placed on strong shock-boundary-layer interaction involving separation. This topic is of particular relevance to high-speed aerospace and turbomachinery aerodynamics. Relevant closure forms and their merits, relative to simpler linear eddy-viscosity approximations, are reviewed first, mainly in qualitative terms. The performance of some particular models is then examined by reference to solutions for a range of 2D and 3D compressible flows.

Keywords: Compressible flow; Shock/boundary-layer interaction; Turbulence modelling; Non-linear eddy-viscosity models; Reynolds-stress closure

1. Introduction

The aerodynamic behaviour of a high-speed flow over a carefully streamlined aerodynamic body or turbomachine blade operating at its design condition is usually dictated by a balance of inviscid processes, with turbulence playing an important role only in the thin, normally attached layer developing on the component's surface and in the component's wake. The prevalence of such flows in aerospace and turbomachinery, in which a single shear strain dominates the flow structure, has promoted the formulation and use of 'simple' algebraic, one-equation and two-equation eddy-viscosity turbulence models which are carefully tuned to return the correct level of shear stress – the only one of importance to the mean flow in the shear layer. There are, however, important sets of circumstances in which the near-wall structure of high-speed flows is much more complex, and in which turbulence can materially affect, directly or by indirect interaction, the aerodynamic performance of the component in question.

The most challenging conditions arise in transonic and supersonic flows in which shocks interact with boundary layers, causing substantial changes not only to the boundary layers themselves, but also to inviscid portions of the flow. Although shock systems can be highly complex, especially if provoked by obstacles subjected to supersonic flow (Fig. 1(a)), the most frequent case involves a single incident shock (Fig. 1(b)) – for example, over a wing in transonic flow, on a ramp in supersonic flow or in a passage formed by blades in which the flow is choked.

Viewed in terms of boundary-layer properties, a shock may be regarded, essentially, as a region of steep adverse pressure gradient causing rapid deceleration. The details of the interaction itself are not trivial, even in the (nominally) 2D normal-shock conditions shown in Fig. 1(b): the shock splits into an oblique leg and a weaker normal leg, giving it the appearance of a 'lambda'. The oblique leg is the one primarily interacting with the boundary layer, causing it to thicken and possibly separate. Following the oblique shock, the flow above the thin region very close to the wall finally decelerates to a subsonic state through the weak normal leg of the lambda-shock structure. If the incident shock is sufficiently strong, the boundary layer separates, and there arises a long and relatively thin recirculation region which has a profound effect on the pressure distribution on the wall and which substantially affects the shock position. Thus, the interaction has important viscous as well as inviscid elements. In 3D conditions, some very complex interaction patterns arise, as will emerge later by reference to computational solutions for a wall-mounted fin and in a swept bump in a channel.

From a computational and modelling point of view, compressible flows, in general, and shock/boundary-layer interaction, in particular, pose substantial challenges. Although some features of this interaction are also encountered in other boundary layers subjected to smoothly varying adverse pressure gradient, there are aspects which make the prediction of shock-affected flows especially difficult. There is, first, the question of numerical accuracy and shock-capturing in a mixed elliptic/hyperbolic flow in which the representation of acoustic characteristics is of considerable importance. Modern implicit upwind methods, based on bounded, Riemann-solver

* Corresponding author. Tel.: +44-161-200-3704; fax: +44-161-200-3733.

E-mail address: m.leschziner@umist.ac.uk (M.A. Leschziner).

0142-727X/00/$ - see front matter
PII: S0142-727X(00)00006-0

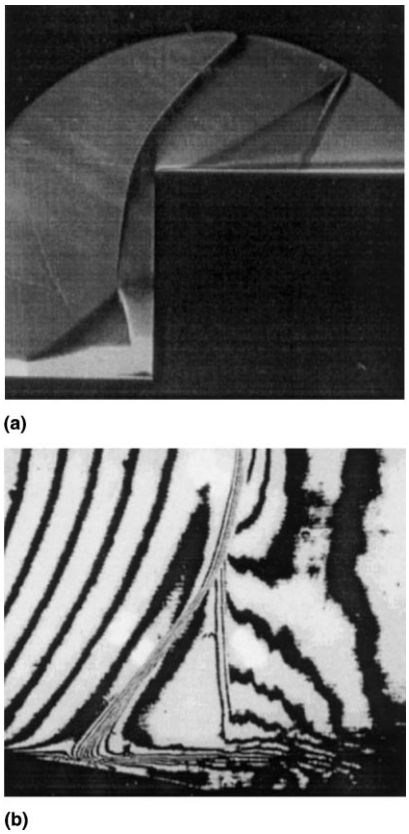

Fig. 1. Visualisation of complex shock/boundary-layer interactions (Figs. courtesy J. Délery, ONERA). (a) Schlieren photograph, (b) Density interferogram.

technology and higher-order characteristic interpolation, are now generally regarded as offering an accurate and stable numerical framework. However, their complexity, especially when applied to general 3D turbulent flows, has encouraged the use of simpler, arguably less adequate approaches, such as Jameson-type methods, and compressibility-extended SIMPLE-type schemes, the latter originally formulated for incompressible, elliptic flow.

As regards turbulence, one important process is the large normal straining associated with the shock in the transonic part of the flow and the steep compression/expansion waves in the subsonic boundary layer. Both cause turbulence to be generated in proportion to the product of streamwise normal stress and normal strain. Hence, turbulence anisotropy, which is observed to be especially high in the interaction region, can be expected to exert a material influence on the turbulence energy. While the response of the boundary layer to the shock is dictated, principally, by the level of the shear stress, this level is sensitive to both the turbulence energy and normal-stress anisotropy. This is especially so if separation is provoked, in which case anisotropy-related curvature/turbulence interaction in the separated shear layer can be expected to influence the reattachment process and post-reattachment recovery.

Another potentially influential issue is the sensitivity of the eddy structure (e.g. spanwise boundary-layer streaks), the cascade mechanism and the dissipative processes to compressibility, in general, and shocks, in particular. It is well known that the spreading rate of a shear layer reduces substantially with increasing Mach number beyond about $M = 0.7$. These observations suggest a suppressing effect of compressibility on turbulence, although the reasons for this influence remain largely unclear. Morkovin (1987) hypothesised that a lack of upstream and transverse signal propagation would cause a reduction in communication across the shear layer and hence a reduction in the the growth of shear-layer instabilities. Breidenthal (1992) has elaborated on this hypothesis with the concept of 'sonic eddies' – turbulent eddies whose rotational Mach number may exceed unity even when the mean flow is still subsonic. As the Mach number increases, so does the proportion of these eddies, whose local domain of dependence prevents the usual entrainment of fluid and turbulent mixing processes. While one might expect a similar sensitivity to prevail near a wall, this is not, in fact, borne out by DNS studies (Huang et al., 1995; Friedrich and Bertolotti, 1997) and modelling efforts (Huang et al., 1994), and this has been linked to the very different levels of turbulence anisotropy in free and wall-bounded shear layers, especially the low level of wall-normal fluctuations.

In view of the above considerations, one might assume that only the most elaborate turbulence models, specifically those resolving anisotropy and its interplay with the shear stresses, would be able to give an adequate representation of the complex interaction processes in shock-affected flows. However, the long history of using simple models in aerospace, the desire for economy and robustness, and the fact that, even in complex separated conditions, the turbulence-affected shear layers tend to remain relatively thin and to occupy a minor proportion of the whole flow, have combined to encouraged an ethos of devising flow-class-specific extensions to models formulated, principally, for near-equilibrium, incompressible, attached shear layers, so as to make the models applicable to much more complex strain fields. The success of this approach has been distinctly mixed.

There have been a number of substantive validation exercises aiming to categorize the performance of a wide variety of models for compressible flows. Several CEC-funded projects are among them, e.g. EUROVAL (Haase et al., 1993), ETMA (Dervieux et al., 1998) and ECARP (Haase et al., 1996). Moreover, a recent ERCOFTAC Workshop focused specifically at 2D shock-boundary layer interaction (Batten et al., 1997). Perhaps the most definitive – certainly most carefully controlled – set of studies was undertaken by Bardina et al. (1997a) (see also Huang, 1997). This examined, in great detail, the performance of four substantially different eddy-viscosity models for a range of flows, including several incompressible and compressible thin shear flows, and two transonic flows with shock-induced separation (bump flow (Bachalo and Johnson, 1986), the RAE 2822 aerofoil (Cook et al., 1979)). Of the models investigated, only the shear-stress-transport (SST) variant of Menter (1994) – a blend between the k–ϵ and the k-ω models – performed adequately in respect of shock/boundary-layer interaction. However, like other eddy-viscosity models, this is unable to capture anisotropy and the multiplicity of associated effects, and its favourable performance reflects careful tuning and the introduction of a shear-stress limiter. This latter feature is extremely influential because, as already noted, the shear-stress level is the key to predicting the mean flow in what essentially remains, despite the separation zone, a thin shear flow.

Extensive experience with modelling a wide range of incompressible flows (e.g. Leschziner, 1994; Hanjalič, 1994), demonstrates that, in complex strain associated with strong curvature, swirl, separation and impingement, anisotropy-resolving closures often return distinctly superior performance to that of isotropic eddy-viscosity models. Some limited experience with 'simple' second-moment models (high-Re variants using linear pressure–strain proposals) applied to shock-induced separation (e.g. Benay et al., 1987; Huang, 1990; Leschziner et al., 1993; Leschziner, 1993; Lien and Leschziner,

1993; Vandromme and Haminh, 1985) suggests improvements over conventional eddy-viscosity models similar to those achieved with Menter's SST variant. To a degree, these improvements reflect the fact that second-moment closure implies, in simple shear, a value for the eddy-viscosity coefficient C_μ which is somewhat lower than the standard value 0.09. Similarly, the SST model partly derives its favourable characteristics from a reduction in C_μ through its functional dependence on the vorticity magnitude. While this might be interpreted as an argument in favour of using 'corrected' linear eddy-viscosity models, it must be borne in mind that the improved performance of such models is tied up with the peculiar nature of relatively simple, thinly separated flow regions. More complex cases, involving 3D straining and impingement, are far more challenging, and it is arguable that only general approaches, involving higher-order closure practices, are likely to have a wide range of applicability.

This paper reviews some recent studies which aimed to assess the predictive performance of non-linear eddy-viscosity and full second-moment-closure models for compressible 2D and 3D flows, with particular emphasis placed on shock-induced separation. Importantly, these efforts did not simply confine themselves to the complex applications of principal interest, but followed a route starting with homogeneous flows and progressing through a sequence of increasingly complex 2D and finally 3D flows. It turns out, as is almost invariably the case with turbulence-modelling studies, that conclusions on predictive performance cannot be stated in simple, monochromatic terms. Nor is it possible to track down unambiguously what precise mechanisms are responsible for particular improvements or predictive characteristics; any model is a 'package' rather than a simple superposition of fragments. All that can be offered, at present, is a cautiously favourable view of anisotropy-resolving models on the basis of a wide-ranging validation.

2. Modelling issues

2.1. Effect of compressibility on turbulence

Virtually all turbulence models in existence have been derived and calibrated, at least in their original form, by reference to incompressible flows. Hence, an issue which needs to be addressed before any particular model variant is considered in detail, is the effect of compressibility on the turbulence equations. This is greatly aided by the availability of direct numerical simulations of compressible boundary layers (Coleman et al., 1995) shear flow (Vreman et al., 1996; Blaisdell et al., 1993) and isotropic turbulence passing through shocks (Hannappel and Friedrich, 1995; Mahesh et al., 1995; Lee et al., 1997) which have provided important insight into the fundamental mechanisms at play. Most importantly, in the present context of predicting compressible boundary layers with statistical models, they have yielded crucial information on the validity of compressibility corrections to turbulence closures formulated for incompressible flow.

Although the effects of compressibility are all interlinked, they may be considered in two parts, the first dealing with spatial mean-density variations and the second with consequences arising from temporal density fluctuations in turbulence correlations.

Mean-density variations are accounted for, as matter of course, in the computation of the convective as well as diffusive fluxes, the latter through dilatation terms in the constitutive stress-strain relations, for example. What is normally not accounted for, however, are effects of density variations on the numerical values of the turbulence-model coefficients. Thus, Huang et al. show that satisfaction of the van Driest compressible *log*-law of the wall depends on the use of the ratio of local-to-wall densities in deriving the universal velocity $U^+ = f(y^+)$. This has implications to the manner in which numerical constants in the turbulence-transport equations are derived by reference to experiments for incompressible flows. For example, the well-known turbulence–equilibrium relationship between the constants in the dissipation-rate equation C_{ϵ_1}, C_{ϵ_2}, the von Kàrmàn constant κ and the Prandtl number for the turbulence dissipation σ_ϵ, which is used to fix C_{ϵ_1}, depends, in compressible conditions, on the density gradients, and failure to account for this link leads to errors in the representation of the boundary-layer structure. One difficulty here is that every model variant, even within the same model category, exhibits a different level of sensitivity to the density gradient. Marvin and Huang, 1996 show, for example, that the k–ω model is much less sensitive than the k–ϵ model to the density gradient, at least in terms of the log-law of the wall. Another problem is that the interaction of mean-density gradients with turbulence-model constants cannot really be divorced from other interactions associated with density fluctuations, for which explicit compressibility corrections are usually introduced. Hence, the effects of mean-density gradients need to be investigated on models which are complete, i.e. with all compressibility corrections included. Fortunately, mean-density effects appear to be relatively unimportant when the Mach number is below 2–3.

The effects of compressibility on turbulence transport, via density fluctuation, emerges upon a consideration of the equations governing the Reynolds stresses. This is normally done using density-weighted averaging. Compressibility manifests itself, explicitly, through the appearance of density–velocity (''turbulent mass-flux'') and density-temperature correlations in the momentum and energy equations

$$\bar{\rho}\widetilde{u_i''} = -\overline{\rho' u_i'}, \qquad \bar{\rho}\widetilde{T''} = -\overline{\rho' T'} \tag{1}$$

dilatational pressure–strain and dilatational dissipation fragments in the Reynolds-stress equations

$$\Phi_{ij}^{(d)} = \frac{2}{3}\overline{p'\frac{\partial u_k'}{\partial x_k}}\delta_{ij}, \tag{2}$$

$$\varepsilon_{ij}^{(d)} = \frac{4}{3}\bar{\nu}\overline{s_{kk}' s_{ll}'} \tag{3}$$

and pressure–work terms which contain the turbulent mass flux

$$\bar{\rho}\widetilde{M_{ij}} = -\overline{\rho u_i''}\frac{\partial p}{\partial x_j} - \overline{\rho u_j''}\frac{\partial p}{\partial x_i}. \tag{4}$$

Moreover, there are covert influences which appear upon the expansion of density-weighted correlations in terms of conventional Reynolds averages. For example,

$$\begin{aligned} \bar{\rho}\widetilde{u_i'' u_j''} \quad &\Big\{ = \overline{\rho u_i' u_j'} - \overline{\rho u_i'' u_j''} + \overline{\rho' u_i' u_j'} \Big\}, \\ \bar{\rho}\widetilde{u_i'' T''} \quad &\Big\{ = \overline{\rho u_i' T'} - \overline{\rho u_i'' T''} + \overline{\rho' u_i' T'} \Big\} \end{aligned} \tag{5}$$

contain the turbulent mass fluxes as well as triple correlations associated with density fluctuations. Finally, variations in mean density are important, of course.

Morkovin's Hypothesis (Morkovin, 1962), applicable to supersonic boundary layers at $M < 5$, suggests that normalized pressure and total-temperature fluctuations are small, and that density fluctuations are linked, principally, to temperature fluctuations which are related, in turn, to Mach number and velocity via,

$$\frac{T'}{T} \approx -(\gamma - 1)M^2 \frac{u'}{\bar{u}}. \tag{6}$$

This allows a number of important simplifications to be introduced in transonic flows. Thus, the correlations (1) can be safely ignored, which simplifies (5) and removes (4). Also, Huang et al. (1994) show that $\overline{\rho' u_i' u_j'}$ in (5) is of order 3% and 10% of $\bar{\rho}\widetilde{u_i'' u_j''}$ in boundary layers at $M = 1.5$ and 3, respectively, with maxima close to the wall. This leaves open the question of the importance of the dilatational pressure and dissipation terms.

There have been several proposals over the past decade for modelling the dilatational dissipation terms (Zeman, 1990; Sarkar et al., 1991; Wilcox, 1993; Fauchet et al., 1997) and the pressure–strain fragments (Aupoix et al., 1986; Sarkar, 1992; Zeman, 1993; El Baz and Launder, 1993). While the models differ substantially in detail, most use the turbulent Mach number (usually squared) as a key indicator of the importance of compressibility. All models were derived by reference to flows unaffected by walls (homogeneous or free-shear flows), and their applicability to near-wall flows was unclear until the analysis of DNS data by Huang et al. (1995) for supersonic boundary layers at $M = 1.5$ and 3 demonstrated that the dilatational terms are insignificant in near-wall flows, in marked contrast to free flows. Huang et al. also showed that all major models for the dilatational terms grossly over-estimate their actual influence, and that the assumption of the dilatational dissipation being correlated with the turbulent Mach number is incorrect. Indeed, the effect of most compressibility corrections on turbulent boundary layers is in the wrong direction (Huang, 1990). It is not surprising, therefore, that the use of these models to predict compressible boundary layers gives disappointing results. Thus, the outcome of extensive validation studies in the 1990s at NASA for shock-affected boundary layer interaction is encapsulated in the following statement by Marvin and Huang (1996): "indeed experience has shown that for the prediction of subsonic and supersonic flows, these two modifications degrade the results and are not recommended".

While the profound difference in the level of contribution of the dilatational terms in free and wall-bounded flows is not fully understood, Friedrich and Bertolotti (1997) conjecture, on the basis of a linear analysis of Coleman et al. (1995) DNS data, that the primary source is the impermeability constraint of the wall and its damping influence on wall-normal velocity fluctuations. A parameter which appears to be particularly influential is the gradient Mach number Sl/c (where S is the strain, l is the integral length scale of turbulence and c is the speed of sound) which is one order of magnitude higher in free-shear layers than in boundary layers.

In view of the current state of knowledge, outlined above, no compressibility corrections have been used in computations reported later.

2.2. Second-moment closure

All second-moment models consist, in essence, of transport equations (or simplified algebraic approximations thereof) for the individual components of the Reynolds-stress tensor

$$\frac{\partial \bar{\rho}\widetilde{u_i'' u_j''}}{\partial t} + \frac{\partial \bar{\rho}\widetilde{u_i'' u_j''}\widetilde{u}_k}{\partial x_k} = P_{ij} + d_{ij} + \phi_{ij} - \epsilon_{ij}. \tag{7}$$

All share one common key element: the (formally) exact representation of stress generation, P_{ij}, which is of primary importance for predicting anisotropy and the distinctly different levels of sensitivity of turbulence to different types of strains. Despite this commonality, there are important differences among second-moment models, especially in respect of pressure–strain interaction, ϕ_{ij}, and rate of dissipation, ϵ_{ij}, which can have a decisive impact on their predictive performance.

The most basic form of second-moment closure is that of Launder et al. (1975) or Gibson and Launder (1978) which is applicable to fully established turbulence only and employs a linear approximation for the pressure–strain terms, in combination with influential near-wall corrections, and an isotropic rate of dissipation. This is by far the most intensively investigated form for complex flows, and variants of this model have also been applied to shock-affected flows, either in conjunction with wall functions or low-Re eddy-viscosity models for the semi-viscous near-wall region (e.g. Vandromme et al., 1983; Davidson, 1995; Lien and Leschziner, 1993; Leschziner et al., 1993). An overall conclusion emerging from these studies is that second-moment closure predicts a higher level of sensitivity of boundary layers to strong shocks, relative to k–ϵ eddy-viscosity models, the former being in closer accord with reality.

In itself, this conclusion is perhaps not of pivotal importance, since, as stated in Section 1, linear eddy-viscosity models can be modified to yield correspondingly good predictions (Bardina et al., 1997b). What is important, however, are the implications for more complex flows involving impingement, separation, complex 3D strain and high curvature, where all Reynolds stresses are dynamically active and contribute in equal measure to momentum transport. Unfortunately, it is here that limitations of the above simple second-moment models can become constraining – specifically, their reliance on influential near-wall correction, which contain wall-normal distances, and on lower-order near-wall models to represent viscous effects.

Recent developments in second-moment modelling have focused on two areas: non-linear approximations for the pressure–strain and stress-dissipation processes, aiming to correctly steer the stresses and the related dissipation rates towards the two-component wall limit, without large topography-related wall corrections, and on extensions to low-Re conditions. While several low-Re second-moment models have been proposed in recent years, some linear (Jakirlič and Hanjalič, 1995; Shima, 1993; Shima, 1997) and others non-linear (Launder and Tselepidakis, 1993; Launder and Li, 1994; Craft and Launder, 1996; Speziale et al., 1993), these have not been widely adopted, and only a few applications to complex non-attached flows have been undertaken. Even rarer are studies of shock-affected flows with such closure forms (Batten et al., 1999a,b; Vallet and Gerolymos, 1996), mainly because of numerical difficulties, associated especially with the near-wall region, and the high resource requirements.

Recent work at UMIST (e.g. Launder and Li, 1994; Craft and Launder, 1996) has focused on the design of low-Reynolds-number closures which represent adequately the near-wall state with much weaker explicit wall corrections, owing to the use of a cubic pressure–strain model. In what follows we have used a variant of the cubic pressure–strain model, obtained originally by Fu et al. (1985) from imposed constraints such as symmetry, tensorial consistency, zero-trace and satisfaction of the two-component limit. In the construction of this model, extensive use is made of the stress invariants

$$A_2 = a_{ij}a_{ij}, \quad A_3 = a_{ij}a_{jk}a_{ki}, \quad A = 1 - 9/8(A_2 - A_3). \tag{8}$$

The last of these invariants – Lumley's *stress-flatness parameter*, A (Lumley, 1978) – has the especially useful property of assuming the value 1 in isotropic turbulence and 0 in the two-component limit. Whilst much more elaborate than the early linear forms, this non-linear model offers improved predictive characteristics in a variety of complex strain fields. Some inhomogeneity corrections are still included to obtain the best possible prediction of the near-wall anisotropy, but these do

not involve wall-normal distances or vectors, relying rather on the local, normalised length-scale gradients (Craft and Launder, 1996)

$$d_i^A = \frac{N_i^A}{\frac{1}{2} + (N_k^A N_k^A)^{1/2}}, \quad N_i^A = \frac{\partial(k^{3/2}A^{1/2}/\epsilon)}{\partial x_i}. \tag{9}$$

The vector, d_i^A, which provides information on both the direction and magnitude of inhomogeneities, is used to modify the 'slow' part of the pressure-strain model. In particular, d_i^A become unit 'normal-to-wall' vectors close to a solid surface where the length scale and flatness parameter undergo significant changes in the wall-normal direction.

The above model, calibrated by reference to incompressible flow, was initially found to give rise to serious anomalies when applied to shock-containing flows. Specifically, terms relying on A for steering turbulence towards the two-component limit were found to respond to shocks as though they were walls, thus shutting off the redistribution process and causing a prediction of a two-component-limit state of turbulence downstream of strong shock waves. Hence, a number of specific modifications have been found necessary in compressible flow fields (Batten et al., 1999a,b). Among them, a modified dissipation equation has been adopted, using the length-scale moderator term proposed by Iacovides and Raisee (1987), and inhomogeneity corrections are damped by a function which vanishes as the turbulence approaches an isotropic state, thus avoiding non-physical damping of the streamwise-normal stresses across a shock wave.

2.3. Non-linear eddy-viscosity models

Predictive inadequacies of linear eddy-viscosity models observed for many years in computations of complex flows have motivated the introduction of numerous corrections into these models in efforts to extend their applicability, thus avoiding the use of second-moment closure. Such corrections have included a functionalisation of the coefficients $C_{\epsilon 1}$ or $C_{\epsilon 2}$ in the dissipation-rate equation to curvature- or buoyancy-related gradient or flux Richardson numbers (e.g. Rodi, 1979), sensitising the eddy-viscosity coefficient C_μ to curvature strain, strain invariants and turbulence-production-to-dissipation ratio P_k/ϵ (e.g. Rodi and Scheuerer, 1983; Rodi, 1976; Leschziner and Rodi, 1981; Cotton and Ismael, 1995; Menter, 1994) and giving different weights to normal and rotational straining in the rate of production of dissipation (Hanjalič and Launder, 1979). While these corrections undoubtedly yielded predictive improvements, their generality was somewhat limited, for they simply addressed specific symptoms rather than their fundamental source – the linear stress-strain relations coupled with the isotropic eddy viscosity. While second-moment closure was well understood to offer a far superior modelling foundation, there was (and still is) much reluctance to use this closure form, because of its complexity, the numerical challenges it poses, the variability in performance of different variants and persistent uncertainties in the modelling of the influential pressure–strain and dissipation terms, especially in low-Re flow.

Against the above background, the quest for simplicity and computational economy has motivated, in recent years, the development and use of non-linear eddy-viscosity models which are able to resolve some of the interactions described by second-moment closure. Such models have their origin in the work of Lumley (Lumley, 1970; Lumley, 1978) and in Pope's (1975) early explicit form of the Reynolds-stress closure from which transport terms are excluded. Indeed, several much newer forms have been derived along a route involving successive simplifications to Reynolds-stress-transport models (Gatski and Speziale, 1993; Taulbee and Sonnenmeier, 1993; Apsley and Leschziner, 1998).

The starting point of several other non-linear models (e.g. Shih et al., 1993; Craft et al., 1996), has been the general non-linear, explicit expansion for the Reynolds-stress tensor in terms of the strain and vorticity tensors, the linear truncation of which gives the conventional Boussinesq relations. While expansions of any order can be proposed, in principle, the most general formulation depends on a finite number of tensorially independent groups, and its coefficients are functions of a finite number of tensorial invariants, owing to the Cayley–Hamilton theorem. The most general cubic constitutive relationship for the Reynolds stresses may be written in the following canonical form:

$$\begin{aligned}\frac{\widetilde{u_i u_j}}{k} - \frac{2}{3}\delta_{ij} = & -2C_\mu f_\mu S_{ij} + a_1\left(S_{ik}S_{kj} - \frac{1}{3}S_{kl}S_{lk}\delta_{ij}\right) \\ & + a_2(W_{ik}S_{kj} - S_{ik}W_{kj}) + a_3\left(W_{ik}W_{kj} - \frac{1}{3}W_{kl}W_{lk}\delta_{ij}\right) \\ & + (b_1 S_{kl}S_{lk} + b_2 W_{kl}W_{lk})S_{ij} \\ & + b_3\left(W_{ik}W_{kl}S_{lj} + S_{ik}W_{kl}W_{lj} - \frac{2}{3}S_{kl}W_{ln}W_{nk}\delta_{ij}\right) \\ & + b_4(W_{ik}S_{kl}S_{lj} - S_{ik}S_{kl}W_{lj}),\end{aligned} \tag{10}$$

which contains non-linear products of the vorticity and strain tensors

$$W_{ij} = \frac{1}{2}\frac{k}{\epsilon}(U_{i,j} - U_{j,i}) \quad \text{and} \quad S_{ij} = \frac{1}{2}\frac{k}{\epsilon}(U_{i,j} + U_{j,i} - \frac{2}{3}U_{k,k}\delta_{ij})$$

with coefficients being functions of strain and vorticity invariants

$$S = \sqrt{2S_{ij}S_{ij}} \quad \text{and} \quad \Omega = \sqrt{2W_{ij}W_{ij}}.$$

The principal merit of relation (10) is that the quadratic terms allow anisotropy to be described, while the cubic terms allow the model to be sensitised to the effects of streamline curvature and swirl. However, the quality with which these interactions are represented depends greatly on the coefficients which are typically derived by calibration against experimental or DNS data for key flows. This is well brought out in Fig. 3 and Table 1 which give, respectively, distributions of normal stresses predicted by four models (k–ϵ – Launder and Sharma, 1993; WR – Wilcox and Rubesin, 1981; CCS – Craft et al., 1996; AL – Apsley and Leschziner, 1998) in a fully developed channel flow at $Re = 5500$ in comparison with DNS data of

Table 1
Equilibrium values for homogeneous shear flow

	$(a_{11})_\infty$	$(a_{12})_\infty$	$(a_{22})_\infty$	$(a_{33})_\infty$	$(Sk/\varepsilon)_\infty$
Experimental	0.403	−0.284	−0.295	−0.108	6.08
k–ϵ	0	−0.434	0	0	4.82
WR	0.300	−0.434	−0.300	0	4.82
CLS	0.530	−0.273	−0.307	−0.223	7.66
AL	0.449	−0.276	−0.353	−0.095	6.81

Kim et al. (1987) and limiting stress values in homogeneously strained turbulence. Clearly, there is a considerable variability among models, and this reflects a decisive sensitivity to calibration.

An important feature in most non-linear models is the dependence of the coefficient C_μ (associated with the linear term) on the stress and strain invariants. This dependence, shown in Fig. 2, for four models, is quite strong and plays a decisive role in the response returned by the models to normal straining (e.g. in impinging flow) and is also influential in shear flow, especially at large strain rates. Importantly, as the non-dimensional strain $(k/\epsilon)\partial U/\partial y$ exceeds the equilibrium value of 3.33, C_μ drops significantly. This condition arises especially in flows subjected to normal straining, among them decelerating boundary layers. Hence, with C_μ reducing, the eddy viscosity declines, and a boundary layer subjected to adverse pressure gradient is more likely to separate. This might be interpreted as suggesting that linear models, incorporating strain-dependent C_μ functions might be satisfactory substitutes for non-linear models. While this is indeed a defensible proposition in some simple flows, in which curvature is weak and in which the normal stresses are not dynamically active, it is not the case in complex strain. Moreover, it may be shown that, at least in one model (Apsley and Leschziner, 1998), C_μ depends on the cubic fragments, even in simple shear, while this interdependence arises in all models in the presence of curvature (Apsley et al., 1998).

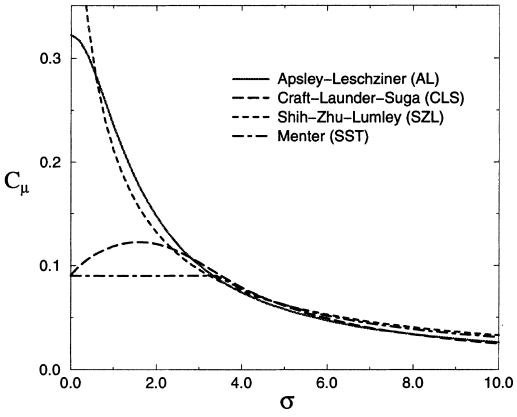

Fig. 2. Variation of C_μ with $\sigma = (k/\epsilon)(\partial U/\partial y)$.

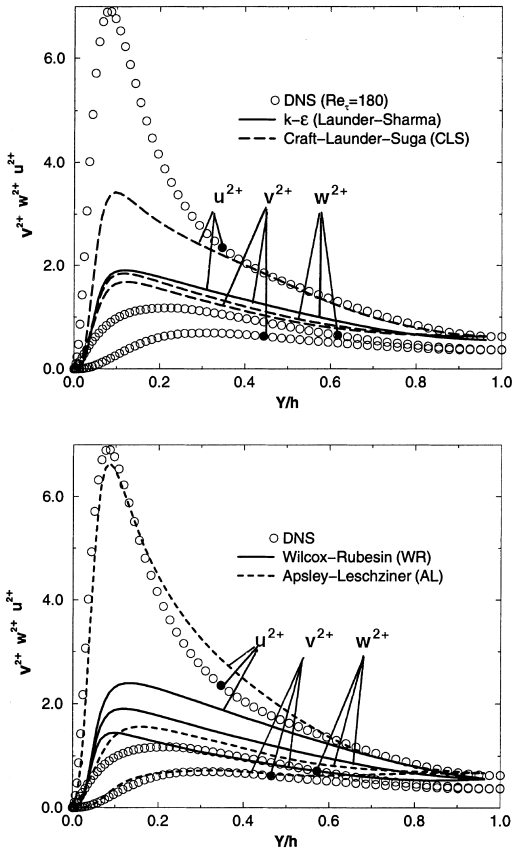

Fig. 3. Plane channel flow–turbulent normal stresses.

3. Some applications

Over the past three years, the writers have been engaged in studying the performance of second-moment and non-linear eddy-viscosity models by reference to a number of shock-affected flows for which well-regarded experimental data exist. Geometries considered included nominally 2D cases, such as Délery's (1981) channel bump, Bachalo and Johnson's (1986) axisymmetric bump, several transonic jet/afterbody flows, supersonic flow around a plate-mounted fin (Barberis and Molton, 1995) and Pot et al.'s (1991) 3D skewed channel bump. This section presents a small selection of results to underpin some tentative conclusions presented at the end.

It is important to point out first that the models used herein for compressible flows had been examined, as part of broad-ranging validation efforts, by reference to a sequence of increasingly complex flows, starting from homogeneous strain (plain, axi-symmetric and shear) and progressing through channel flow to impinging jet flow and finally transonic and supersonic flow. Space constraints preclude, except for one example, results arising from initial incompressible-flow studies to be included herein; the interested reader is referred to Batten et al. (1999a), Loyau et al. (1998) and Batten et al. (1999b). These same references also contain much broader expositions of compressible-flow results than can be included herein.

Perfect two-dimensionality has been assumed in computations for nominally two-dimensional geometries. While there can be little argument about the validity (indeed, unavoidability) of this practice in the axi-symmetric cases considered here, there is some uncertainty in relation to the plain geometries – for example, Délery's bump flow – which inevitably feature some spanwise variations. Here, a 3D solution would be an option, in principle, albeit at the penalty of an enormous increase in computing cost and reduced resolution in the primary plane. The principal 3D effects arise from the boundary layers on the spanwise walls and their interaction with the curved flow associated with surface curvature and separation. The latter, in particular, inevitably leads to some spanwise secondary motion in the interaction region. Preliminary 3D computations with relatively coarse grids for the nominally 2D Délery bump have shown, however, that the influence of 3D features on the flow are minor over most of its spanwise extent, and that the 2D resolution reflects well the structure of the flow in that region.

Computations presented below have been performed with an implicit HLLC Riemann-solver-based upwind scheme (Batten et al., 1997). Both non-linear and second-moment models pose particular stability problems within this low-diffusion numerical framework. Quadratic and higher-order terms in a non-linear tensorial expansion contribute a large and potentially de-stabilising source if added explicitly, whilst

a full linearisation of all higher-order terms makes the implementation of the more complex non-linear eddy-viscosity models an expensive task. Second-moment models are notorious for being numerically 'brittle'. This is partly due to a natural stiffness in the equations, but is also often due to the prediction (at least in early transients) of non-realisable stress data. One of the most frequent causes of instability is the violation of normal-stress positivity or the shear-stress Schwartz inequality, and this provides a strong motivation for the use of a non-linear, realisable, pressure–strain model. The present approach solves the set of mean-flow conservation equations implicitly and the turbulence equations implicitly as a separate subset. The subsets are partially (block-) coupled through the use of apparent viscosities (see Huang and Leschziner, 1995).

Prior to presenting examples for shock-affected flow, attention is directed briefly to an incompressible flow, namely a round air jet discharging from a smooth pipe and impinging on a flat plate fixed perpendicular to the pipe axis (Cooper et al., 1993). The main purpose of presenting this case is to highlight the importance of representing correctly the sensitivity of turbulence to irrotational straining associated with stagnation flow. Fig. 4 shows profiles of normal-stress and mean velocity predicted by four models: the modified Craft–Launder Reynolds-stress model (MCL) (Batten et al., 1999a,b), the Launder and Sharma (1993) k–ϵ model (k–ϵ), the SST variant (SST) of Menter (1994) and the Jakirlič and Hanjalič (1995) Reynolds-stress model (JH). The most noticeable defects occur with the linear eddy-viscosity models in the stagnation region. Moving away from the centre-line in the radial direction, the cubic Reynolds-stress model displays better agreement than the linear JH variant. This is due, in part, to known weaknesses with the conventional wall-reflection terms used in the latter model (see, for example, Craft and Launder, 1992). Earlier computations by Ince and Leschziner (see Leschziner, 1995) for twin-impinging, under-expanded jets at Mach numbers up to 2.6 with Gibson & Launder's linear second-moment closure (Gibson and Launder, 1978) show features broadly consistent with those above.

The first compressible case, frequently used to assess turbulence models, is that of the transonic flow over a plane channel bump, known as Délery (1981) case C. The computations were performed over a clustered 121×121 mesh with the wall-nearest gridline being at $y^+ < 0.5$. Wall-pressure distributions are compared to experimental data in Fig. 6, while Fig. 5 compares predicted iso-Mach contours for seven different models. For this test case, the normal stresses do not contribute significantly to the mean-flow behaviour, and as a result the well-predicted shear stresses obtained with the SST model give a mean-flow solution which is comparable with second-moment closure and the AL-model, the latter being the most sensitive of the non-linear eddy-viscosity models investigated. More comprehensive studies on this case may be found in Batten et al. (1997), Haase et al. (1993), Loyau et al. (1998), Loyau et al. (1998).

The next example was examined experimentally by Bachalo and Johnson (1986) and is essentially the axi-symmetric equivalent of the previous flow. The geometry consists of a cylinder, with a circular arc bump subjected to an $M = 0.875$ flow. A 180×110 grid was used, with clustering applied around the shock and near the wall. Computational results for different models are compared in Fig. 7 with experimental data. The MCL and the AL models are seen to return a considerably more pronounced pressure–plateau region than do other models, predicting a shock location which is

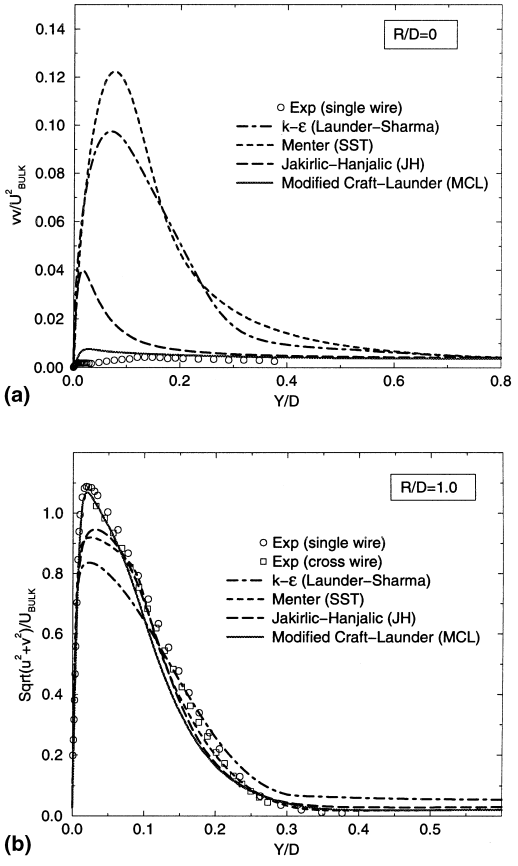

Fig. 4. Impinging jet: axial normal stresses on stagnation line (a) and mean velocity profile at $R/D = 1$ (b).

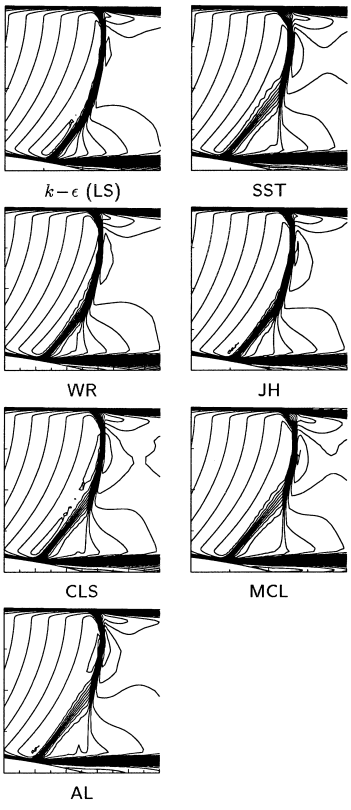

Fig. 5. ONERA bump C: iso-Mach contours.

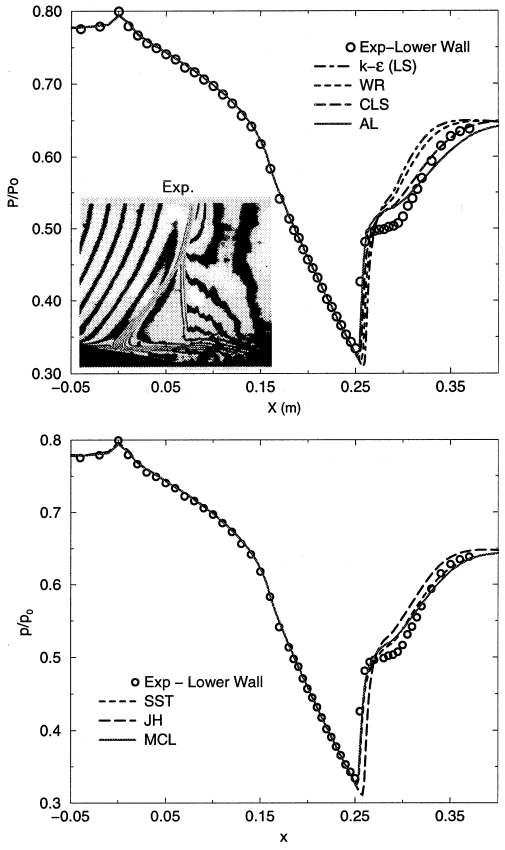

Fig. 6. ONERA bump C: lower-wall pressure distributions.

fractionally too far upstream. Here again, the SST model gives a performance very similar to the best non-linear eddy-viscosity and second-moment models, for reasons discussed in the previous section. Comparisons for velocity or shear-stress profiles may be found in Batten et al. (1999a,b) and Loyau et al. (1998) and are, in terms of sensitivity to the shock, consistent with the results for pressure.

Figs. 8–10 relate to two examples of axi-symmetric afterbody flows. The first example, in Figs. 9 and 8, shows configuration 1 of the NASA-Langley afterbody with a solid plume simulator (see Newbold, 1990). This configuration include a solid metal 'plume' in the base region to simulate the blocking effect of the jet on the outer flow. Fig. 9 shows model comparisons at both subsonic ($M = 0.8$) and supersonic ($M = 1.2$) conditions. In both cases, an explicit Musker velocity profile, using a van Driest compressibility transformation was used to impose an incoming boundary layer of thickness of $0.18D$, with D the (exterior) diameter of the afterbody. Boattail pressure distributions in Fig. 9 demonstrate the improved flow representation obtained with the modified Craft–Launder Reynolds-stress model, relative to that returned by the k–ϵ and the Jakirlić–Hanjalić models. For this case, Menter's SST model gives agreement comparable to that of the present Reynolds-stress model, but owing to quite a different modelling mechanism.

The second afterbody example is taken from a range of configurations studied experimentally by Carson and Lee (1994). This series of tests was designed to cover a range of flight-like conditions, from subsonic acceleration through to supersonic cruise. The high jet-pressure ratios and boattail curvatures in one of the case examined (Case 1) resulted in substantial shock-induced separation of the flow from the boattail region of the afterbody, and these cases are therefore of principal interest herein. An exterior boundary-layer thickness of $0.1D$ was assumed, with D the internal nozzle diameter. Known reservoir conditions and nozzle (total-to-freestream) pressure ratio of 3.09 were prescribed at the jet-exit boundary. The agreement shown in Fig. 10 is good for the interior throat section of both nozzles, suggesting the interior jet flow is essentially governed by inviscid processes. Agreement for the boattail pressure coefficient is variable, with the SST and MCL models correctly predicting a more extensive separation-related pressure plateau.

The final 2D case considered here is the RAE 2822 aerofoil (Cook et al., 1979), shown in Fig. 11. Attention is restricted to 'case 10', in which the shock induces mild separation. The flow conditions are $Re = 6.2 \times 10^6, M_\infty = 0.754$ and incidence $= 2.57°$. This set is the one adopted in the collaborative EUROVAL project (Haase et al., 1993), but it must be noted that studies at NASA (e.g. Bardina et al., 1997a) have used a higher incidence angle which allows better matching of pre-shock pressure on the aerofoil's suction surface, especially at the leading edge. Calculations were performed on a 364×128 grid extending to 30 chords, at which a vortex-corrected far-field boundary condition was applied. Fig. 12 shows comparisons for wall pressure predicted with three models. Here again, the SST model and the MCL second-moment closure return similar predictions. While all models over-predict the post-shock suction pressure and give a shock which is too far downstream, the uncorrected k–ϵ models tend to give the worse agreement (by far).

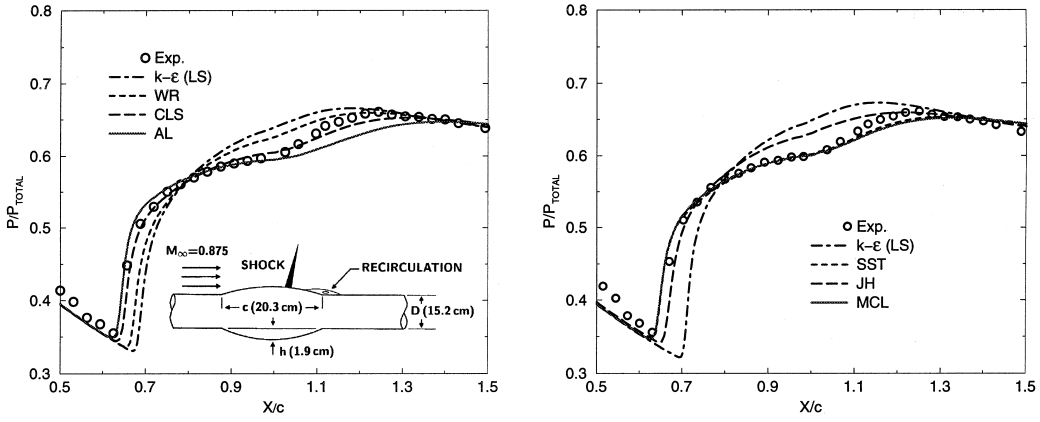

Fig. 7. Axi-symmetric bump: wall-pressure distributions.

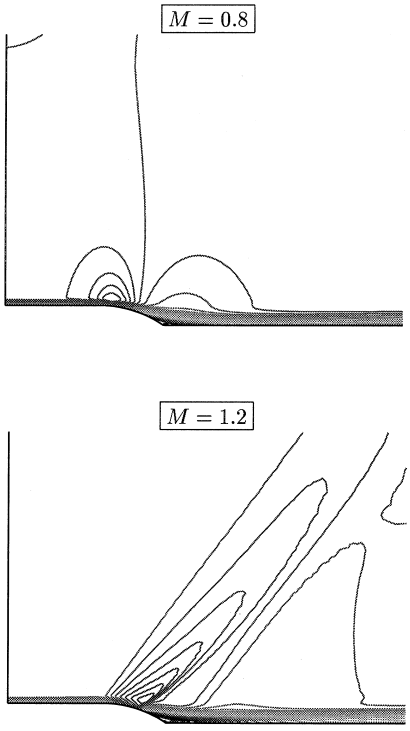

Fig. 8. Langley Case 1: iso-Mach contours.

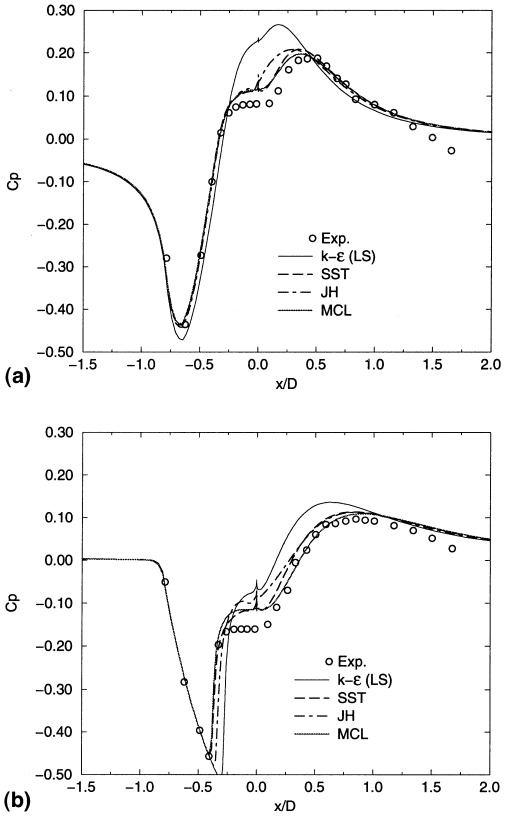

Fig. 9. Langley Case 1: $M_\infty = 0.8$ (a) and $M_\infty = 1.2$ (b).

The first 3D example is that of a Mach 2 flow around a blunt-fin/flat-plate junction. Extensive experimental data for this configuration were obtained at ONERA by Barberis and

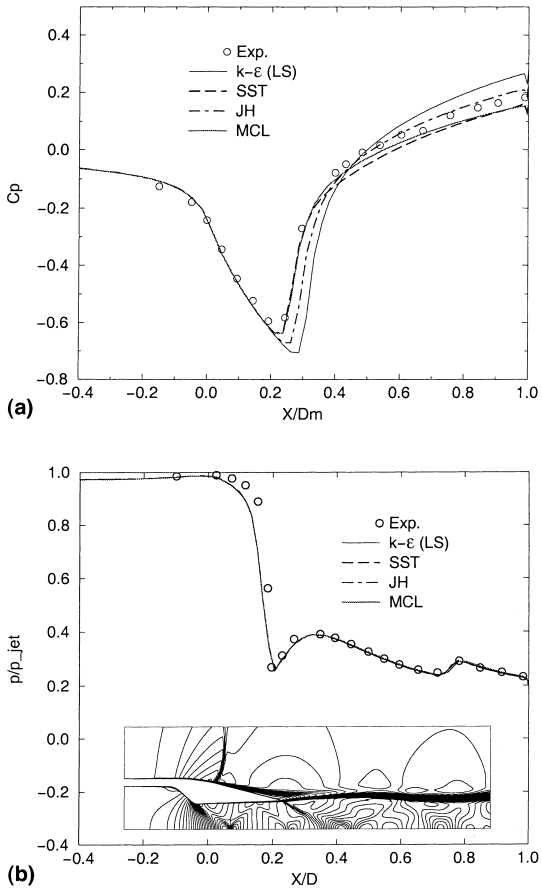

Fig. 10. Carson and Lee configuration 1: boattail Cp (a), iso-Mach contours and internal nozzle p/p^T_{jet} (b).

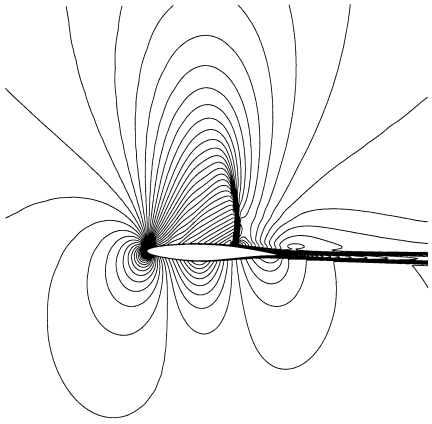

Fig. 11. RAE 2822 Case 10: iso-Mach contours, k–ϵ.

Molton (1995). An $80 \times 80 \times 70$ grid was used to compute this flow, with the mesh clustered at the walls to ensure $y^+ < 1$ everywhere. Fig. 13 gives a general overview of the flow field, as predicted by the SST and MCL models, with stream-tubes identifying virtual-particle paths. The multiple-vortex phenomenon is a key feature of this flow which is missed by the linear SST model. This is most clearly brought out through plots of skin-friction lines (or limiting streamlines) on the wall, which indicate the footprint of the vortices. Such plots may be

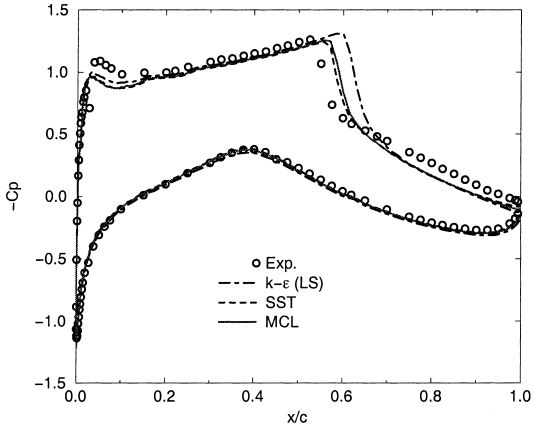

Fig. 12. RAE 2822 Case 10: pressure coefficient distributions.

found in Batten et al. (1999a,b). Wall-pressure plots in Fig. 14 show a rise in pressure following separation, followed by a local minimum, caused by the stronger vortex nearer to the fin surface. Predicted peak pressures in front of the fin are around 5.5 times that of the undisturbed free-stream, but these peaks decay and move downstream as the horizontal traverses move away from the fin in the span-wise direction. Although the MCL model under-predicts the upstream extent of separation, the results are in better agreement than the predictions returned by the linear JH Reynolds-stress model which employs conventional wall-reflection terms.

The final case considered here is the flow over a 60° skewed bump in a channel (Pot et al., 1991). This case is highly challenging, both computationally and physically. As shown in Fig. 15, it requires adequate resolution not only of the first throat creating the supersonic flow ahead of the bump, but also a second downstream throat used to control the flow-rate. Physical complexities arise from the strongly 3D, asymmetric nature of the interaction, giving very different flow patterns at all four confining walls. Computations have been carried out with several linear and non-linear eddy-viscosity models, among them the linear low-Reynolds-number k–ϵ model of Lien and Leschziner (1999) (LL) and the cubic variant thereof by Lien et al. (1996) (LCL) on a grid of $120 \times 55 \times 60$ nodes. Figs. 16 and 17 compare pressure distributions on the lower bump wall and the upper plane wall, respectively, at spanwise positions at or close to the midplane. All that can be said at this time is that at least modest improvements can be gained, especially in the primary shock/boundary-layer interaction region, from using models which are more elaborate than linear eddy-viscosity forms.

4. Concluding remarks

The investigation of turbulence models for compressible flows is subject to many uncertainties arising from numerical issues, the sensitivity of shock position to boundary conditions and the structure of the turbulence-affected parts of flow, the ill-understood effects of compressibility on turbulence and the range and accuracy of experimental data obtained in very challenging flow conditions. These uncertainties militate

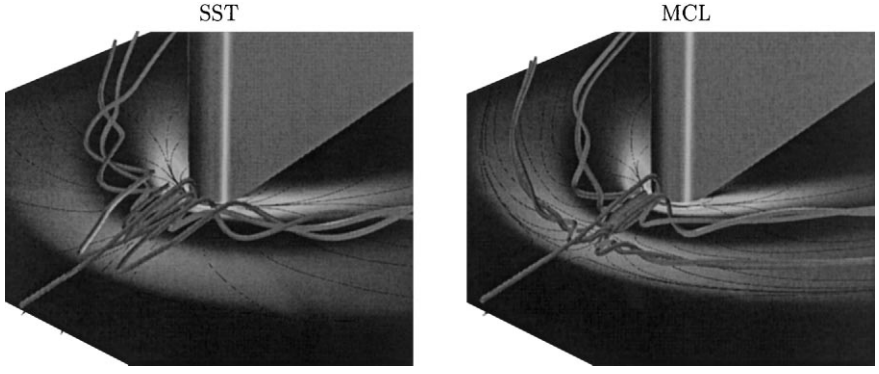

Fig. 13. ONERA blunt-fin: overview of flow-field predictions.

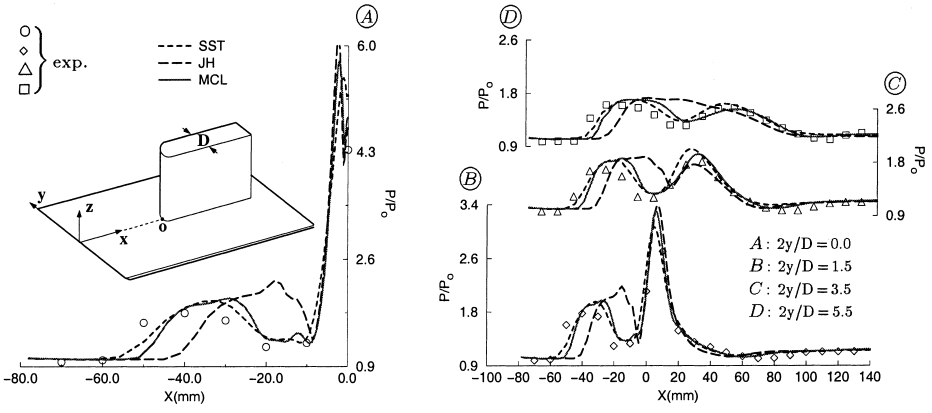

Fig. 14. ONERA blunt-fin: plate pressure distributions – $D = 2$ cm.

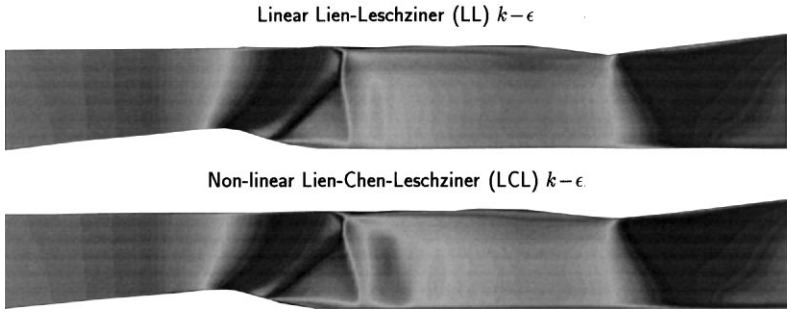

Fig. 15. ONERA skewed bump: iso-Mach contours in the Y-middle plane – full geometry.

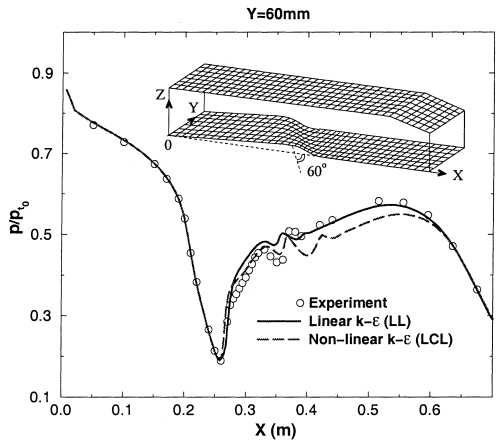

Fig. 16. ONERA skewed bump: upper-wall pressure distributions.

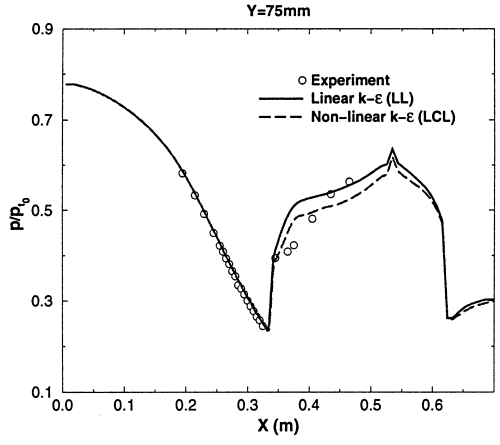

Fig. 17. ONERA skewed bump: lower-wall pressure distributions.

against definitive conclusions being derived even from wide-ranging investigations which encompass several compressible flows and many turbulence models implemented within a single numerical framework, and which are also supplemented by studies for homogeneous and incompressible flows.

The focus of this paper has been on the interaction between shocks and boundary layers. In most cases, especially in 2D flow, this interaction is dominated by a single shear stress, while the influence of the normal stresses is of subordinate importance. In such circumstances, some carefully corrected eddy-viscosity models, such as Menter's SST variant, give results which are, in essence, as good as those obtained with more elaborate anisotropy-resolving closures. However, this equivalence is unlikely to extend to complex 3D flows in which all Reynolds-stress components are influential, and some evidence for this assertion has been provided. At this stage, the body of experience on the very small number of 3D flows for which reasonably detailed experimental data are available does not suffice to make a more definitive statement. Second-moment-closure calculations have now been made for geometries as complex as a generic single-engine fighter model (Batten et al., 1998). However, experimental data for such geometries are limited to surface-pressure profiles, and these do not suffice to assess the relative merits of different turbulence models.

Acknowledgements

The authors are grateful to BAE SYSTEMS and the UK Defence and Evaluation Research Agency (DERA) for their financial support. Some of the calculations presented in this paper were performed with computational resources provided within the framework of the 'Contrat de Plan du Bassin Parisien' (Article 12-Pôle interrégional de modélisation en sciences pour l'ingénieur).

References

Apsley, D.D., Leschziner, M.A., 1998. A low-Re non-linear two-equation turbulence model for complex flows. Int. J. Heat Fluid Flow 19, 209–222.

Apsley, D.D., Chen, W-L, Leschziner, M.A., Lien, F-S., 1998. Non-linear eddy-viscosity modelling of separated flows. IAHR J. Hydraulic Res. 35, 723–748.

Aupoix, B., Blaisdell, G.A., Reynolds, W.C., Zeman, O., 1986. Modelling the turbulent kinetic energy equation for compressible homogeneous turbulence. AIAA J. 24, 437–443.

Bachalo, W.D., Johnson, D.A., 1986. Transonic turbulent boundary-layer separation generated on an axisymmetric flow model. AIAA J. 24, 437–443.

Barberis, D., Molton, P., 1995. Shock wave-turbulent boundary layer interaction in a three dimensional flow. AIAA J. 95-0227.

Bardina, J.E., Huang, P.G., Coakley, T.J., 1997a. NASA TM-110446.

Bardina, J.E., Huang, P.G., Coakley, T.J., 1997b. Turbulence modelling validation. AIAA 97-2121.

Batten, P., Leschziner, M.A., Goldberg, U.C., 1997. Average state Jacobians and implicit methods for compressible viscous and turbulent flows. J. Comp. Phys. 137, 38–78.

Batten, P., Craft, T.J, Leschziner, M.A., Loyau, H., 1999a. Reynolds-stress-transport modelling for compressible aerodynamics applications. AIAA J. 37 (7), 785–797.

Batten. P., Loyau, H., Leschziner, M.A. (Eds.), 1997. In: Proceedings of the ERCOFTAC Workshop on Shock-Wave/Boundary-Layer Interaction, UMIST, Manchester.

Batten. P., Leschziner, M.A., 1998. An implicit multi-block flow solver for compressible turbulent flow. Final BAe Tech. Report, UMIST, Mech. Eng. Dept..

Batten. P., Leschziner, M.A., Craft, T.J., 1999b. Reynolds-stress modelling of afterbody flows. In: Proceedings of the First Symposium on Turbulence and Shear Flow. Phenomena, Santa Barbara (to appear).

Benay, R., Coët, M.C., Délery, J., 1987. A study of turbulence modelling in transonic shock-wave/boundary-layer interactions. In: Proceedings of the Sixth Turbulence Shear Flows, Toulouse, pp. 8.2.1–8.2.6.

Blaisdell, G.A., Mansour, N.N., Reynolds, W.C., 1993. Compressibility effects on the growth and structure of homogeneous turbulent shear flow. J. Mech. Engrg. 256, 443–485.

Breidenthal, R., 1992. Sonic eddy – a model for compressible turbulence. AIAA J. 30, 101–104.

Carson, T.J., Lee, E.E. Jr., 1994. Experimental and Analytical Investigation of Axisymmetric Supersonic Cruise Nozzle Geometry at Mach numbers From 0.60 to 1.30. NASA TM-108827.

Coleman, G.N., Kim, J., Moser, R.D., 1995. A numerical study of turbulent supersonic isothermal wall channel flow. J. Fluid Mech. 305, 159–183.

Cook, P.H., McDonald, M.A., Firmin, M.C.P., 1979. Aerofoil 2822-Pressure distributions, boundary layer and wake measurements. AGARD AR-138.

Cooper, D., Jackson, D.C., Launder, B.E., Liao, G.X., 1993. Impinging jet studies for turbulence model assessment, Part1: Flow-field experiments. Int. J. Heat Mass Transfer 36, 2675–2684.

Cotton, M.A., Ismael, J., 1995. Some results for homogeneous shear flows computed using a strain parameter model of turbulence. In: Proceedings of the 10th Turbulence Shear Flows. Pennsylvania State University, pp. 26-7–26-12.

Craft, T.J., Launder, B.E., 1996. A Reynolds-stress closure designed for complex geometries. Int. J. Heat Fluid Flow 17, 245–254.

Craft, T.J., Launder, B.E., 1992. New wall-reflection model applied to the turbulent impinging jet. AIAA J. 30, 2970–2972.

Craft, T.J., Launder, B.E., Suga, K., 1996. Development and application of a cubic eddy-viscosity model of turbulence. Int. J. Heat Fluid Flow 17, 108–115.

Davidson, L., 1995. Reynolds stress transport modelling of shock induced separated flow. Comput. and Fluids 24, 253–268.

Délery, J., 1981. Investigation of strong turbulent boundary-layer interaction in 2D flows with emphasis on turbulence phenomena. AIAA 81–1245.

Dervieux, A., Braza, F., Dussauge, J-P., 1998. Computation and Comparison of Efficient Turbulence Models for Aeronautics – European Research Project ETMA, Notes on Numerical Fluid Mechanics, Vol. 65, Vieweg.

El Baz, A.M., Launder, B.E., 1993. Second-moment modelling of compressible mixing layers. In: Engineering Turbulence Modelling and Experiments 3. Elsevier, Amsterdam, pp. 63–70.

Fauchet, G., Sho, L., Wunenberger, R., Bertoglio, J.P., 1997. An improved two-point closure for weakly compressible turbulence and comparison with large-eddy simulations. Appl. Sci. Res. 57, 165–194.

Friedrich, R., Bertolotti, F., 1997. Compressibility effects due to turbulent fluctuations. Appl. Sci. Res. 57, 165–194.

Fu, S., Launder, B.E., Tselepidakis, D.P., 1985. Accomodating the effects of high strain rates in modelling the pressure–strain correlation. Rep. TFD/87/5, UMIST, Department of Mechanical Engineering, Manchester.

Gatski, T.B., Speziale, C.G., 1993. On explicit algebraic stress models for complex turbulent flows. J. Fluid Mech. 254, 59–78.

Gibson, M.M., Launder, B.E., 1978. Ground effects on pressure fluctuations in the atmospheric boundary-layer. J. Fluid Mech. 86, 491–511.

Haase, W., Brandsma, F., Elsholz, E., Leschziner, M.A. and Schwamborn, D., 1993. EUROVAL – A European Initiative on Validation of CFD Codes, Notes on Numerical Fluid Mechanics, vol. 42, Vieweg Verlag.

Haase, W., Chaput, E., Elsholz, E., Leschziner, M.A. and Muller, U.R., 1996. ECARP II – Validation of CFD Codes and Assessment of Turbulence Models. Notes on Numerical Fluid Mechanics, vol. 58, Vieweg Verlag.

Hanjalič, K., Launder, B.E., 1979. Preferential spectral transport by irrotaional straining. ASME J. Fluids Engrg. 102, 34–40.

Hanjalič, K., 1994. Advanced turbulence closure models: a view of current status and future prospects. Int. J Heat Fluid Flow 15, 178–203.

Hannappel, R., Friedrich, R., 1995. Direct numerical simulation of a Mach 2 shock interacting with isotropic turbulence. Appl. Sci. Res. 54, 205–221.

Huang, P.G., Leschziner, M.A., 1995. Stabilization of recirculating-flow computations performed with second-moment closures and third-order discretization. In: Proceedings of the Fifth Symposium on Turbulence Shear Flow. Cornel, pp. 20.7–20.12.

Huang, P.G., Bradshaw, P., Coakley, T.J., 1994. Turbulence models for compressible boundary-layers. AIAA J. 32, 735–740.

Huang, P.G., 1997. Turbulence models for compressible boundary layers. In: Proceedings of the ASME FED Summer Meeting, 22–26 June.

Huang, P.G., Coleman, G.N., Bradshaw, P., 1995. Compressible turbulent channel flows – DNS results and modelling. J. Fluid Mech. 305, 185–218.

Huang, P.G., 1990. Modelling hypersonic boundary-layer flows with second-moment closure. In: CTR, University of Standford, Annual Research Briefs, pp. 1–13.

Iacovides, H., Raisee, M., 1997. Computation of flow and heat transfer in a 2-D rib roughned Passages. In: Hanjalič, K., Peters, T.W.J. (Eds.), Proceedings of the Second International Symposium on Turbulence, Heat and Mass Transfer. Delph University Press, pp. 21–30.

Jakirlič, S., Hanjalič, K., 1995. A second-moment closure for non-equilibrium and separating high- and low-Re-number flows. In: Proceedings of the 10th Turbulence Shear Flows. Pennsylvania State University, pp. 23.25–23.30.

Kim, J., Moin, P., Moser, R., 1987. Turbulence statistics in fully developed channel flow at low Reynolds number. J. Fluid Mech. 177, 137–166.

Launder, B.E., Reece, G.J., Rodi, W., 1975. Progress in the development of Reynolds-stress turbulence closure. J. Fluid Mech. 68, 537–566.

Launder, B.E., Sharma, B.I., 1993. Application of energy-dissipation model of turbulence to the calculation of flow near a spinning disc. Lett. Heat Mass Transfer 1, 131–138.

Launder, B.E., Tselepidakis, D.P., 1993. Contribution to the Modelling of Near-Wall Turbulence. In: Turbulent Shear Flows 8. Springer, Berlin pp. 81–96.

Launder, B.E., Li, S-P., 1994. On the elimination of wall-topography parameters from second-moment closure. Phys. Fluids 6, 999–1006.

Lee, S., Lele, S.K., Moin, P., 1997. Interaction of isotropic turbulence with shock waves: effects of shock strength. J. Fluid Mech. 340, 225–247.

Leschziner, M.A., 1995. Computation of aerodynamics flows with turbulence transport models based on second-moment closure. Comput. Fluids 24, 377–392.

Leschziner, M.A., 1994. Refined turbulence modelling for engineering flows. In: Comp. Fluid Dynamics'94. Wiley, New York, pp. 33-46.

Leschziner, M.A., Dimitriadis, K.P., Page, G., 1993. Computational modelling of shock wave/boundary layer interaction with a cell-vertex scheme and transport models of turbulence. Aeronaut. J. 97, 43–61.

Leschziner, M.A., Rodi, W., 1981. Calculation of annular and twin parallel jets using various discretization schemes and turbulence models. ASME J. Fluids Engrg. 103, 352–360.

Leschziner, M.A., 1993. ONERA Bumps A and C. In: EUROVAL-An European Initiative on validation of CFD Codes, Notes on Numerical Fluid Mechanics 42, 185–265.

Lien, F.S., Leschziner, M.A., 1993. A pressure–velocity solution strategy for compressible flow and its application to shock/boundary-layer interaction using second-moment turbulence closure. J. Fluids Engrg. 115, 717–725.

Lien, F.S., Leschziner, M.A., 1999. Computational modelling of a transitional turbine – cascade flow using a modified low-Re k–ϵ model and a multi-block scheme. Int. J. CFD 12, 1–15.

Lien, F.S., Chen, W.L., Leschziner, M.A., 1996. Low-Reynolds-number eddy-viscosity modelling based on non-linear stress-strain relations. In: Rodi, W., Bergeles, G. (Eds.), Engineering Turbulence Modelling and Experiments 3. Elsevier, Amsterdam, pp. 91– 100.

Loyau, H., Batten, P., Leschziner, M.A., 1998. Modelling shock/boundary-layer interaction with nonlinear eddy-viscosity closures. J. Flow, Turbulence Combust. 60, 257–282.

Loyau, H., Vandromme, D., 1998. TC5 Synthesis. In: Computation and Comparison of Efficient Turbulence Models for Aeronautics-European Research Project ETMA. Notes on Numerical Fluid Mechanics 65. Vieweg Verlag, pp. 456–471.

Lumley, J.L., 1970. Towards a turbulent constitutive relation. J. Fluid Mech. 41, 413–434.

Lumley, J.L., 1978. Computational modelling of turbulent flows. Adv. Appl. Mech. 18, 123–176.

Mahesh, K., Lee, S.K., Moin, P., 1995. The interaction of an isotropic field of accoustic waves with a shock wave. J. Fluid Mech. 300, 383–407.

Marvin, J.G., Huang, P.G., 1996. Tubulence modelling-progress and future outlook. In: Proceedings of the 15th Conference on Numerical Methods in Fluid Dynamics. Monterey, CA, June.

Menter, F.R., 1994. Two-equation eddy-viscosity models for transonic flows. AIAA J. 32, 1598–1605.

Morkovin, M.V., 1962. Effects of compressibility on turbulent flows. In: Favre, A. (Ed.), Mécanique de la Turbulence. Gordon and Breach New York, pp. 367–380.

Morkovin, M.V., 1987. Transition at hypersonic speeds. In: NACA CR 178315, ICASE Interim Report No. 1.

Newbold, C.M., 1990. Solution to the Navier–Stokes equations for turbulent, transonic flows over axisymmetric afterbodies. In: ARA TR 90–16 (unpublished).

Pope, S.B., 1975. A more general effective-viscosity hypothesis. J. Fluid Mech. 72, 331–340.

Pot, T., Délery, J., Quélin, C., 1991. Interaction choc-couche limite dans un canal tridimensionnel-Nouvelles expériences en vue de la validation du code CANARI. ONERA TR-92/7078 AY.

Rodi, W., 1979. Influence of buoyancy and rotation on turbulent length scale. In: Proceedings of the Second Symposium on Turbulence Shear Flows. London, pp. 10.37–10.42.

Rodi, W., Scheuerer, G., 1983. Calculation of curved shear layers with two-equation models of turbulence. Phys. Fluids 26, 1422–1436.

Rodi, W., 1976. A new algebraic relation for calculating the Reynolds stresses. Z. Angew. Math. Mech. 56, 219–221.

Sarkar, S., Erlebacher, G., Hussaini, M.Y., Kreiss, H.O., 1991. The analysis and modelling of dilatational terms in compressible turbulence. J. Fluid Mech. 227, 473–493.

Sarkar, S., 1992. The pressure–dilatation correlation in compressible flows. Phys. Fluid 282, 163–186.

Shih, T-H., Zhu, J., Lumley, J.L., 1993. A realizable Reynolds stress algebraic equation model. NASA TM-105993.

Shima, N., 1993. Prediction of turbulent boundary layers with a second-moment closure: Part I-effects of periodic pressure gradient, wall transpiration and free-stream turbulence. ASME J. Fluids Engrg. 115, 56–69.

Shima, N., 1997. low-reynolds-number second-moment closure without wall-reflection redistribution terms. In: Proceedings of the 11th Symposium on Turbulence Shear Flows. Grenoble, pp. 712–717.

Speziale, C.G., Sarkar, S., Gatski, T.B., 1993. Modelling the pressure – strain correlation of turbulence: an invariant dynamical system approach. J. Fluid Mech. 227, 245–272.

Taulbee, D.B., Sonnenmeier, J.R., Wall K.M., 1993. Application of a new non-linear stress-strain model to axisymmetric turbulent swirling flows. In: Rodi, W., Martinelli, F. (Eds.), Engineering Turbulence Modelling and Experiments 2. Elsevier, Amsterdam, pp. 103–112.

Vallet, I., Gerolymos, G.A., 1996. near-wall reynolds-stress 3D transonic flow computation. In: Comp. Fluid Dynamics'96. Wiley, New York, pp. 167–173.

Vandromme, D., Haminh, H., Viegas, J.R., Rubesin, M.R., Kollman, W., 1983. second-order closure for the calculation of compressible wall-bounded flows with an implicit Navier–Stokes solver. In: Proceedings of the Fourth Symposium on Turbulence Shear Flows. Karlsruhe, pp. 1.1–1.6.

Vandromme, D., Haminh, H., 1985. In: Délery, J. (Ed), Turbulent Shear-Layer/Shock-Wave Interactions. Springer, Berlin, pp. 127–136.

Vreman, A.W., Sandham, N.D., Luo, K.H., 1996. Compressible mixing layer growth rate and turbulence characteristics. J. Fluid Mech. 320, 235–258.

Wilcox, D.C., Rubesin, M.W., 1981. Progress in turbulence modelling for complex flow field including effects of compressibility. NASA TP-1517.

Wilcox, D.C., 1993. Turbulence Modelling fort CFD, DCW Industries, La Canada, CA.

Zeman, O., 1990. Dilatation dissipation: the concept and application in modelling compressible mixing layers. Phys. Fluids 2, 178–188.

Zeman, O., 1993. New model for super/hypersonic turbulent boundary layers. AIAA 93-0897.